nature neuroscience

A spatiotemporal coding mechanism for background-invariant odor recognition

Debajit Saha[1,2], Kevin Leong[1,2], Chao Li[1,2], Steven Peterson[1], Gregory Siegel[1] & Baranidharan Raman[1]

Sensory stimuli evoke neural activity that evolves over time. What features of these spatiotemporal responses allow the robust encoding of stimulus identity in a multistimulus environment? Here we examined this issue in the locust (*Schistocerca americana*) olfactory system. We found that sensory responses evoked by an odorant (foreground) varied when presented atop or after an ongoing stimulus (background). These inconsistent sensory inputs triggered dynamic reorganization of ensemble activity in the downstream antennal lobe. As a result, partial pattern matches between neural representations encoding the same foreground stimulus across conditions were achieved. The degree and segments of response overlaps varied; however, any overlap observed was sufficient to drive background-independent responses in the downstream neural population. Notably, recognition performance of locusts in behavioral assays correlated well with our physiological findings. Hence, our results reveal how background-independent recognition of odors can be achieved using spatiotemporal patterns of neural activity.

Sensory stimuli often evoke temporal patterns of spiking activity across a population of neurons in the early processing stages[1–12]. These neural responses are considered to be a 'temporal code' if they change on a timescale that is different than the stimulus variations that caused them and when they convey useful information about the stimulus[13]. A fundamental problem in sensory neuroscience is determining what stimulus-specific information is encoded by dynamic patterns of ensemble neural activity and whether this information is behaviorally relevant. Furthermore, because the same stimulus can be encountered in a variety of ways in natural environments, what attributes of the spatiotemporal population responses are invariant to any or all such variations?

The insect olfactory system is a widely used model for studying odor coding and behavior[14–18]. In this system, odorants are detected by olfactory receptor neurons (ORNs) in the antenna, which transduce chemical stimuli into trains of action potentials. The ORN signals are relayed downstream to the antennal lobe, where spatiotemporal patterns of activity across ensembles of projection neurons represent odors. The odor-evoked projection neuron responses are elaborate and change most rapidly after stimulus onset and offset (referred to as on-transient and off-transient responses, respectively). For lengthy odor presentations, the antennal lobe activity converges to a steady state within ~1.5 s of stimulus onset[19–21]. These dynamic neural activity patterns are repeatable across trials and contain information about odor identity and intensity[22–24].

Time-varying response patterns are maximally informative during transient phases of neural activity[20]. Odor representations are most distinct during these epochs and predominantly drive spiking activity in downstream neurons[16,20]. Consistent with these physiological results, behavioral data have indicated that animals are capable of discerning between 'similar' odors (a relatively difficult task) within a few hundred milliseconds of stimulus onset[25–28]. Taken together these results suggest that initial segments of the on-transient response contribute substantially to encoding odor identity.

What then is the importance of neural activity that follows the initial response segment? In the olfactory system, even a very brief odor pulse (lasting a few hundred milliseconds) can generate an elaborate response that lasts for a few seconds. This prolonged stimulus-evoked activity appears to be more of a liability than a feature, as it could potentially interfere with and corrupt the olfactory system's response to other chemical cues in the environment. Two previous studies[24,29] that examined this issue reported results that are rather contrasting. Whereas pulses of the same stimulus generated ensemble activity that was reliable and repeatable at the population level, overlapping pulses of different stimuli created spatiotemporal responses that often interfered with each other heavily, thus making them unpredictable. In both cases, however, the activity was not reset to baseline levels before responses to the freshly introduced stimuli began.

The existence of hysteresis in the olfactory system[29] poses a conundrum, as it may hinder any coding scheme that uses dynamic patterns of neural activity. Yet spatiotemporal patterns of neural activity are ubiquitous in vertebrate[2,6,12,23,30,31] and invertebrate[1,15,19,21,22,24,32] olfactory systems. What role does neural activity patterned over time have in encoding odors? Do response dynamics aid or hinder the rapid detection of new odors in multistimulus environments? We examined these issues using the locust olfactory system.

RESULTS

Stimulus sequences to probe the robustness of odor codes

We sought to systematically perturb the spatiotemporal responses evoked by an olfactory stimulus. To achieve this objective, we exploited the physiological observation that odor-evoked activity in

[1]Department of Biomedical Engineering, Washington University, St. Louis, Missouri, USA. [2]These authors contributed equally to this work. Correspondence should be addressed to B.R. (barani@wustl.edu).

Received 28 June; accepted 8 October; published online 3 November 2013; doi:10.1038/nn.3570

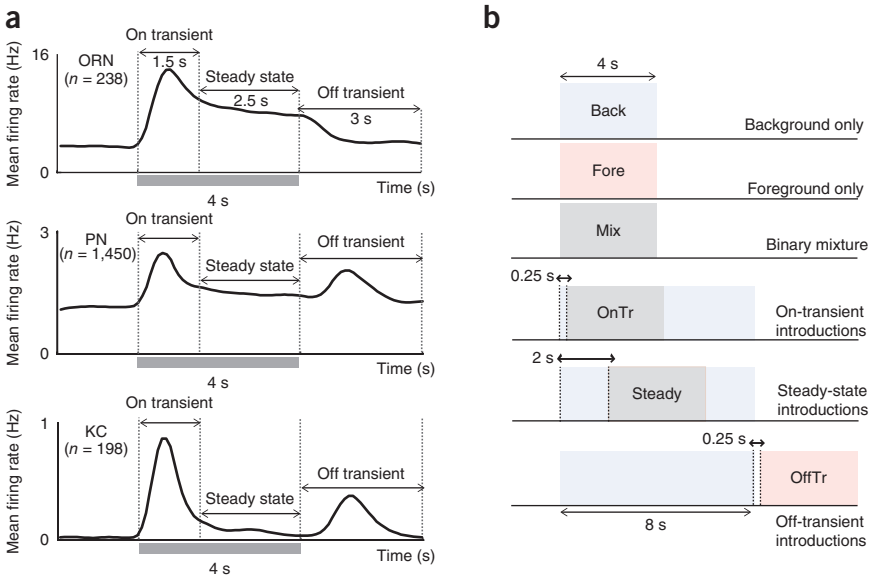

Figure 1 Dynamic states of odor-evoked neural activity. (**a**) Mean firing rates across ORNs, projection neurons (PNs) and Kenyon cells as a function of time are shown (n = 238 ORN-odor combinations; n = 1,450 projection neuron–odor combinations; and n = 198 Kenyon cell–odor combinations). Single neuron activities were determined using extracellular multiunit recordings made at the first three stages of the locust olfactory pathway: antenna, antennal lobe and mushroom body (119 ORNs were recorded from 27 locusts; 725 projection neurons were recorded from 70 locusts; and 99 Kenyon cells were recorded from 39 locusts). The 4-s odor stimulation period is shown as a gray bar along the x axis. In all three neural populations, three dynamical states can be clearly identified: an on-transient response after odor onset, an off-transient response after stimulus termination and a steady-state between the two transient activity phases. (**b**) A schematic representation of the stimulation protocol used (top to bottom): background alone stimulus (Back), foreground alone stimulus (Fore), simultaneous presentation of both the background and the foreground odor (Mix) and foreground odor introductions during the on-transient (OnTr), steady-state (Steady) or off-transient (OffTr) phases of background odor activity.

an ensemble of sensory neurons and their followers in the antennal lobe and mushroom body are in a highly dynamic state after odor onset (for ~1.5 s) and offset (~3 s) (**Fig. 1a** and **Supplementary Fig. 1a–f**). Between these two transient phases, the odor-evoked responses converged to a steady-state activity. Therefore, we used sequences of stimuli where the delay between the onset of the first (background) and second (foreground) odor was varied. We manipulated the foreground odor introductions to occur either concurrently with the background (binary mixture) or during on transients, steady states or off transients of the background odor activity (**Fig. 1b**). This odor stimulation protocol enabled us to probe whether and when the ongoing olfactory network dynamics allow stable representation of a newer stimulus.

To understand the general processing principles that govern how fresh stimulus introductions are tracked by the locust olfactory system, we identified a diverse set of six background-foreground odor combinations (**Supplementary Fig. 1g**). The selected odor pairs included odorants that belong to three groups: (i) the same functional group (background-foreground): 2-octanol–hexanol (2oct-hex) and cyclohexanone–2-heptanone (chex-2hep); (ii) different functional groups: benzaldehyde–isoamyl acetate (bzald-iaa), hexanal-hexanol (hxa-hex) and geraniol-citral (ger-cit); and (iii) a pair of complex blends (mint-apple). This selected stimulus set also accounted for diversity with respect to vapor pressure and relative sensory input strengths, as measured by the electroantennogram signals (**Supplementary Fig. 2**).

Sensory neuron responses to overlapping stimuli

We found that responses to the introduction of the foreground odor in a subset of ORNs remained unchanged regardless of whether they were preceded by a background stimulus (**Fig. 2a**). We commonly observed such reliable responses for those ORNs that responded to the foreground odor only. However, when an ORN responded to both stimuli presented in a sequence or to the background odor only, the spiking activity elicited after introduction of the foreground odor became inconsistent across different conditions (**Fig. 2a**). In some cases, even when the background stimulus did not elicit a response, the ORN spiking activity after foreground odor introduction became diminished because of the presence of the background stimulus (**Fig. 2a**; chex-2hep).

We found that when two odors were presented concurrently, their responses combined in simple ways (**Fig. 2b**). The binary mixture generally elicited a stronger response, as it combined the spiking activities of the component stimuli. The influence of the background odor activity on the foreground odor response diminished as the delay between the onset of the background and foreground odors increased (**Fig. 2c**,**d**). Our results indicate that even though blends of the same two odors were presented, ORN responses could vary depending on the temporal overlap between the two stimuli.

These observations raise the following important question: how similar are the sensory inputs that are generated by the same stimulus under different background and no-background conditions? To understand this issue, we compared the mean number of spikes elicited in a 2-s window after foreground odor onset presented either alone or during different dynamic phases of background odor activity (**Fig. 2c**). We found that the mean spike count changed significantly in a substantial number of ORNs (**Fig. 2c** and Online Methods; $P < 0.05$, d.f. = 4,20, one-way analysis of variance (ANOVA) with Bonferroni correction for multiple comparisons). Compared to the no-background situation, spike counts in most ORNs increased during concurrent, on-transient and steady-state introductions of the foreground stimulus but reduced during off-transient introductions (**Fig. 2d**). Hence, our results show that the same stimulus can generate variable activity across an ensemble of ORNs when presented simultaneously or after a background odor.

Projection neuron responses vary with stimulus history

We then examined whether the variability observed in sensory neuron responses to the same stimulus affected its subsequent processing in the downstream antennal lobe circuits. We made extracellular recordings to monitor the odor-evoked activity in projection neurons that received ORN inputs (n = 725 projection neurons from 70 locusts were recorded, and we included all six odor pairs). We found that projection neuron responses to odor mixtures were more complex.

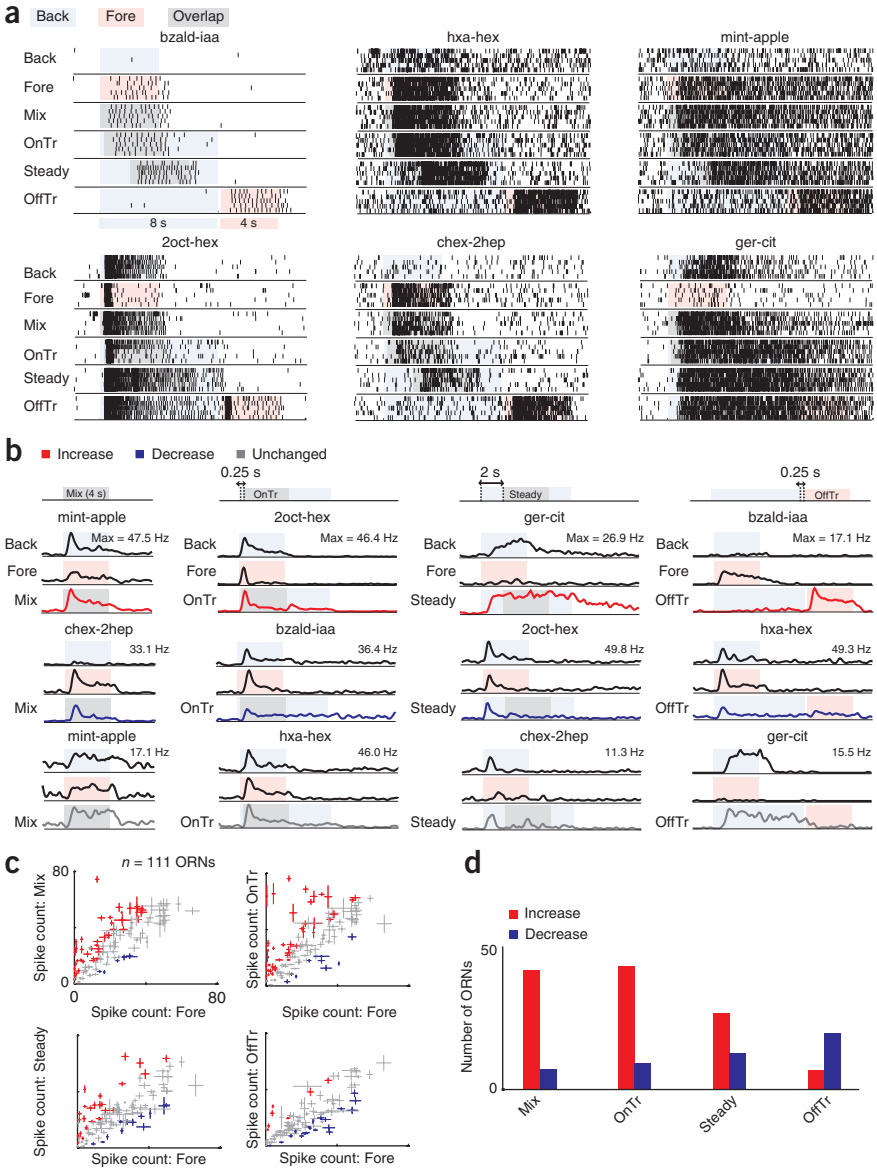

Figure 2 Ongoing background odor-evoked activity interferes with the response of individual sensory neurons to the freshly introduced stimulus. (**a**) Representative raster plots of six ORNs. Each raster plot encompasses six blocks of trials that correspond to the different stimulation conditions shown in **Figure 1b** (in the same order). For each condition, the responses in five trials are shown for assessing repeatability. Colored boxes indicate whether the background and foreground odors were presented alone or in an overlapping fashion. Gray boxes indicate periods of stimulus overlaps. (**b**) PSTHs for representative ORNs (encompassing all six odor pairs) that reveal different ways in which foreground odor responses can change when presented after another stimulus. For each ORN, responses to background and foreground odors (component responses) are shown, along with their response to one of the overlapping conditions. Red, blue and gray PSTHs indicate an increase, a decrease and no significant change, respectively, in the foreground odor response (spike counts) when the same stimulus is presented in a sequence. The maximum firing rate (Max) is specified for each ORN. Each column corresponds to a specific sequence of an odor pair. (**c**) Comparison of mean ORN spike counts in a 2-s window after foreground odor onset. The *x* axis corresponds to spike counts when the foreground odor is presented alone. The *y* axis corresponds to spike counts when the foreground odor is presented after a background stimulus. The mean ± s.e.m. over five trials is shown for all cells. Cells in red indicate a significant increase in spike counts during the overlapping conditions and are therefore located above the diagonal ($P < 0.05$, d.f. = 4,20, one-way ANOVA with Bonferroni correction for multiple comparisons; $n = 111$ ORNs recorded from 27 locusts). Similarly, cells in blue indicate a significant decrease in spike counts, and cells in gray indicate no significant change across the two conditions. (**d**) Total number of ORNs with a significant increase (red) or decrease (blue) in spike counts.

For example, even when both component odors individually increased spiking activity in a projection neuron during odor presentation, their mixture could still reduce activity to below spontaneous levels (**Fig. 3**; PN5). Furthermore, our results indicate that even if the responses to the individual odors were known, it would still not be possible to predict the responses of a substantial number of projection neurons to the same pair of stimuli when presented as a binary mixture or in a sequence (**Fig. 3a**).

We found that nearly 70% of all recorded projection neurons showed substantial deviation from baseline activity after either background or foreground odor introductions ($n = 502$ of the 725 projection neurons recorded; Online Methods). The response evoked by the foreground stimulus in nearly two-thirds of these projection neurons varied depending on the presence or absence of a background odor. We observed interference in overlapping but nonidentical subsets of projection neurons for binary mixture, on-transient, steady-state and off-transient introductions (**Fig. 3a**). For all odor pairs used, we also found a large, nonoverlapping subset of projection neurons that showed reliable responses to the freshly introduced odor under all conditions ($n = 181$ of the 502 projection neurons). Overall our results suggest that it would not be possible to predict whether and how a projection neuron's response to a foreground odor would change with stimulus history.

To systematically quantify these results, we again compared the mean spike counts elicited by the foreground odor presented either alone or after a background odor (**Fig. 3b**; $P < 0.05$, d.f. = 4,45, one-way ANOVA with Bonferroni correction for multiple comparisons). In contrast with the ORN results, the projection neuron activity reduced in general during concurrent, on-transient and steady-state introductions for most of the odor pairs (**Fig. 3b**). Notably, we commonly observed an increase in odor-evoked spiking activity during off-transient introductions. Thus, when encountering a sequence of odorants, projection neuron responses and ORN spiking activity appeared to have an inverse relationship (**Figs. 2d** and **3c**). More importantly, these results clearly show that odor-evoked response patterns in individual projection neurons to a stimulus can change unpredictably in the presence of a background odor.

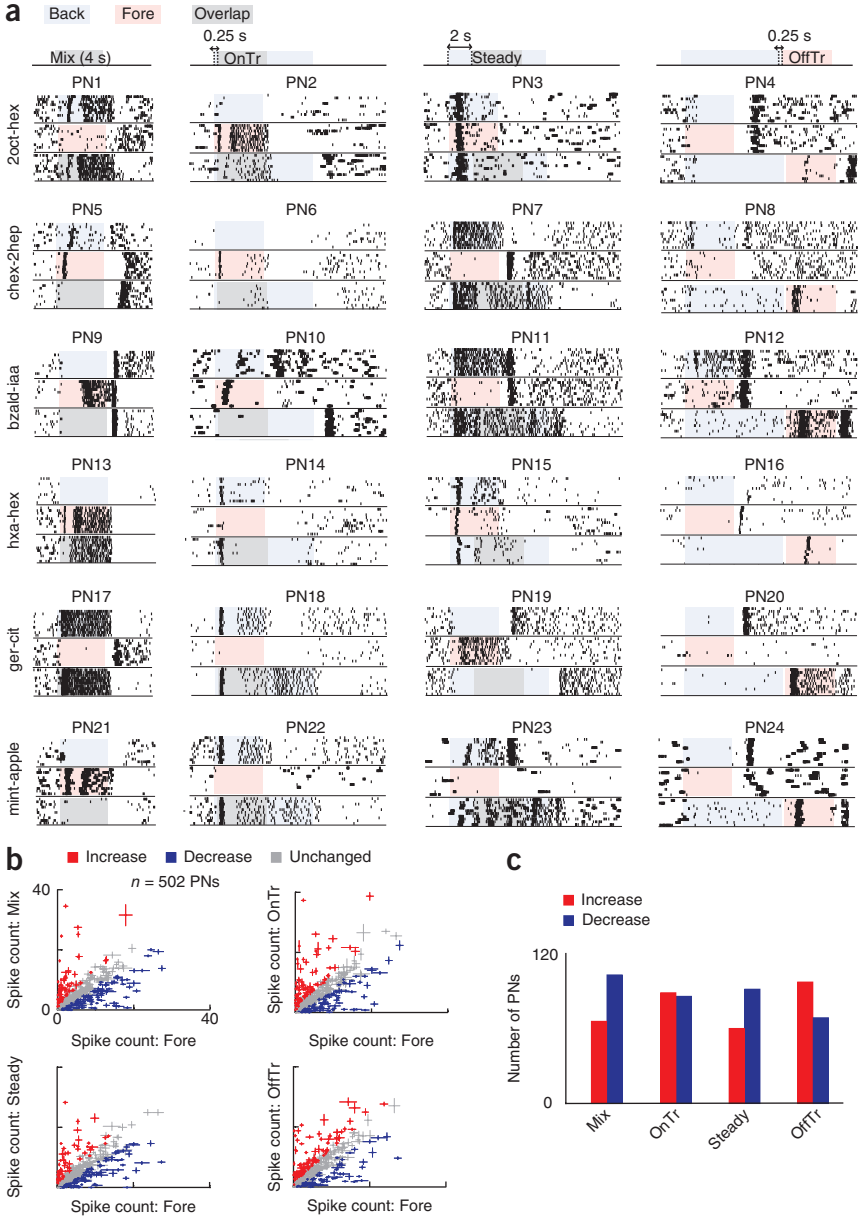

Figure 3 Responses of individual projection neurons to the foreground odor can vary unpredictably depending on stimulus history. (**a**) Representative projection neuron (PN) rasters are shown for all six odor pairs (rows) for different background-foreground sequences (columns). The selected cells clearly reveal that the responses of individual projection neurons (PN1–PN24) receive considerable interference because of ongoing background odor activity. (**b**) Comparison of mean projection neuron spike counts in a 2-s window after foreground odor onsets. The *x* axis corresponds to spike counts when the foreground odor is presented alone. The *y* axis corresponds to spike counts when the foreground odor is presented after a background stimulus. The mean ± s.e.m. over ten trials is shown for all cells. The same analysis and color convention were used as those in **Figure 2c** ($P < 0.05$, d.f. = 4,45, one-way ANOVA with Bonferroni correction for multiple comparisons; $n = 502$ projection neurons recorded from 70 locusts). (**c**) Total number of projection neurons with a significant increase (red) or decrease (blue) in spike counts.

We found that each odorant generated a unique, closed-loop projection neuron response trajectory that returned toward baseline levels within 2 s of odor onset. The binary mixture of two odors generated response trajectories that could be categorized into the following three cases: (i) combined contributions of both components and therefore occupying a region (or subspace) between the two component odors (2oct-hex, chex-2hep and bzald-iaa); (ii) dominated by one component and therefore remaining closer to the stronger component trajectory (hxa-hex and ger-cit); and (iii) evolving over time such that the mixture trajectory moved from one component to the other (mint-apple).

We found that introduction of a foreground stimulus in any of the three different dynamic states of background activity rapidly remapped the antennal lobe activity (**Fig. 4**). In five out of six odor pairs tested (excluding ger-cit), the introduction of the foreground odor during the on-transient phase of the background stimulus caused the projection neuron response trajectory to transition toward the foreground odor response without returning to baseline activity. Foreground odor introductions during steady-state background activity generated response trajectories that evolved from close to baseline responses in a direction that aligned with the foreground odor response. The off-transient introductions of foreground odors also resulted in response trajectories that began close to the baseline response but generated trajectories that were less overlapping for some odor pairs (**Fig. 4**; 2oct-hex, ger-cit and mint-apple). The reorganization of antennal lobe ensemble activity remained qualitatively similar even when we explored additional latencies between background and foreground odor onsets (**Supplementary Fig. 4**). Notably, in all cases, the dynamic reorganization of ensemble activity over time resulted only in partial pattern matches with neural representations evoked by the same foreground stimulus when presented alone.

Dynamic transitions reshape projection neuron ensemble activity

How stable are neural representations for odors distributed across an ensemble of projection neurons? To understand this issue and visualize how projection neuron activity was dynamically reorganized after the introduction of a fresher stimulus, we performed a dimensionality reduction analysis[22,24] (**Fig. 4**). For this analysis, we arranged the ensemble of n projection neuron responses as n-dimensional time-series data ($n = 116$ for 2oct-hex, $n = 104$ for chex-2hep, and so on) over 80 nonoverlapping time bins (i.e., a 4-s odor pulse duration). We then projected the time-varying projection neuron responses onto three dimensions using a nonlinear technique that generated a topology-preserving approximation of the original data set (locally linear embedding[33] (LLE); similar plots using a linear principal components analysis are shown in **Supplementary Fig. 3**). The low-dimensional points were connected in a temporal order to visualize the neural response trajectories generated by different stimuli.

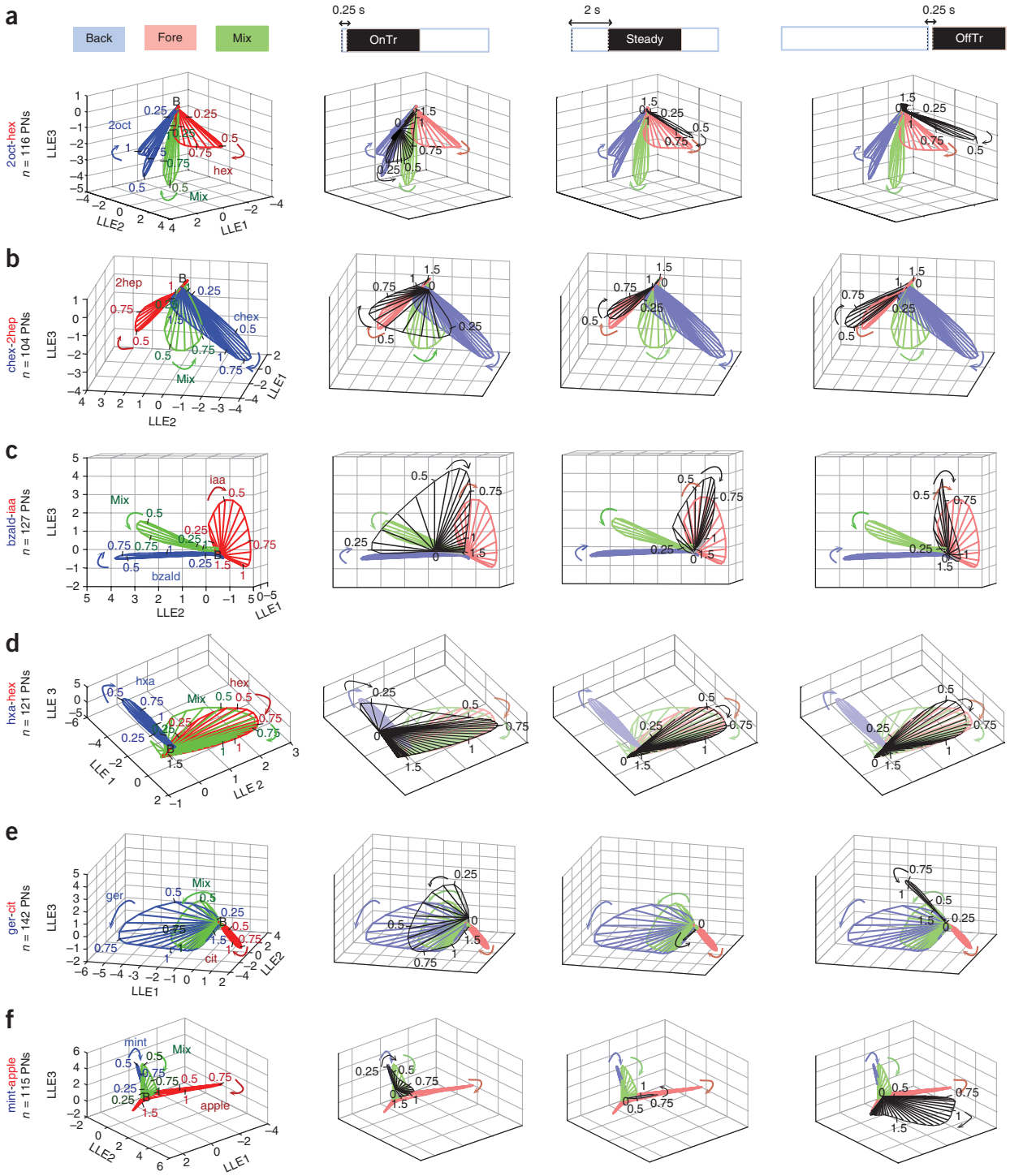

Figure 4 Ensemble projection neuron activity makes dynamic transitions to create response overlaps between neural representations. (**a**–**f**) Odor-evoked projection neuron response trajectories for all six background-foreground odor combinations. Each row represents trajectories corresponding to one particular odor pair, and each column represents one particular sequence of background-foreground odors. Trajectories show the mean projection neuron ensemble response over time along three LLE axes (Online Methods). Numbers on the trajectory show the time since odor onset in seconds. B indicates the baseline activity before odor stimulation. Response trajectories were computed using spike counts in 50-ms nonoverlapping time bins for the 4 s of odor stimulation (80 time-slice data points per stimulus). Odor trajectories are shown for the following three conditions in the left column: background odor (blue), foreground odor (red) and their binary mixture (green). Each stimulus generates a unique closed-loop trajectory after dimensionality reduction. The red, green and blue trajectories are replotted in the other columns, along with the black trajectory that traces the neural activity after foreground introductions during on-transient (second column), steady-state (third column) and off-transient (fourth column) background odor activity ($n = 116$ projection neurons from 34 locusts for 2oct-hex; $n = 104$ projection neurons from 18 locusts for chex-2hep; $n = 127$ projection neurons from 18 locusts for bzald-iaa; $n = 121$ projection neurons from 28 locusts for hxa-hex; $n = 142$ projection neurons from 20 locusts for ger-cit; and $n = 115$ projection neurons from 16 locusts for mint-apple).

Piecewise classification allows robust odor recognition

The dimensionality reduction analysis qualitatively revealed similarities between the spatiotemporal ensemble responses for pure odors and their overlapping sequences. How significant are these observed response overlaps? To investigate this issue, we performed a quantitative, trial-by-trial classification analysis. We considered the high-dimensional ensemble projection neuron firing patterns elicited during solitary foreground and background odor exposures as the desired reference templates to be pattern matched (**Fig. 5a** and Online Methods). Five trial-averaged reference templates were generated for each odor to represent the mean ensemble projection neuron activity in epochs during and immediately after stimulus presentation. Ensemble projection neuron spike counts in trials not used to create reference templates were regarded as test response patterns to be categorized. Each test pattern was subsequently assigned to the category of its best matching reference template (i.e., smallest angular distance).

To limit the classification analysis to meaningful response patterns, we defined two criteria. First, we set a detection threshold to identify significant odor-evoked activity (>2 s.d. of the mean baseline response). Second, we defined a tolerance threshold to identify a meaningful pattern match with reference templates (**Fig. 5a** and Online Methods). We classified only those projection neuron responses that were above the detection threshold and within the similarity tolerance levels. We performed this classification analysis on a bin-by-bin, trial-by-trial basis for all six odor pairs (**Fig. 5b–g**).

We found that a detection threshold that eliminated classification in most prestimulus time bins also limited the classification analysis to the transient periods of antennal lobe activity. These results confirmed observations from trajectory analyses that odor-evoked activities reached close to baseline levels during steady-state epochs.

We found that binary mixture responses that combined contributions from both components (2oct-hex, chex-2hep and bzald-iaa) had significant classification probabilities for both background and foreground odors (**Fig. 5b–d**, and the significance analysis is shown in **Supplementary Fig. 5**). In comparison, when one component dominated the mixture response (hxa-hex and ger-cit), the classification analysis revealed that those responses were more likely to be categorized with only one odor (**Fig. 5e**,**f**). Classification of the mint-apple mixture confirmed the impressions from our trajectory analysis that the response vectors were similar initially to the mint odorant but then evolved over time to pattern match with the apple response (**Fig. 5g**).

Furthermore, similar to results in our trajectory analysis, dynamic introductions of foreground odors atop background odors were detected and recognized during all three dynamic states for all odor pairs except ger-cit. For the on-transient introductions, the classification probabilities changed in a contiguous manner, indicating that the response patterns were more similar initially to the background reference templates but subsequently gained similarity to the foreground odor response. For the steady-state and off-transient introductions, a brief return to the subdetection threshold response allowed the classification periods after the two stimulus onsets to become temporally decoupled (**Fig. 5b–g**). In sum, the classification results matched the qualitative observations from our dimensionality reduction analysis.

Hence, our results suggest that the projection neuron population response, when processed in a piecewise manner, can allow robust recognition of most odors independently of their backgrounds.

Kenyon cells respond robustly to a fresher stimulus

Do the downstream centers that receive input from the antennal lobe take advantage of the dynamic processing of olfactory signals? To examine this question, we first studied the peristimulus time histograms (PSTHs) that combined the activity of all Kenyon cells to each odor used in our study. Consistent with previous results[16,34], we found that Kenyon cells in the mushroom body responded with temporally sparse activity predominantly at odor onset and offset. During the middle portion of a lengthy odor presentation, i.e., during steady-state antennal lobe activity, we found that Kenyon cell firings returned back to baseline levels for all odors tested (**Supplementary Fig. 6**). This result suggests that firing in these cells is limited to those temporal epochs when afferent activity was in a dynamic phase with higher firing rates.

We found that a few Kenyon cells were less selective and responded to both background and foreground odors (44 of 99 Kenyon cells, including KC1 and KC3; **Fig. 6** and Online Methods). Such responses, however, were less common for those odor pairs not belonging to the same functional group (15 of 55 Kenyon cells, including KC5 and KC10). A few Kenyon cells responded to all introductions of a particular foreground odor, suggesting that any partial overlap in the projection neuron ensemble responses was sufficient to drive spiking activity in these cells (for example, KC2, KC5 and KC7). In sum, our results indicate that Kenyon cell responses are consistent with the information content of the projection neuron ensemble responses and that a subset of Kenyon cells can respond to odors independently of the stimulus presented before them.

Predicting behavior from physiology results

Can overlaps observed in antennal lobe ensemble neural activity also predict behavioral recognition of odors? To investigate this issue, we assessed the recognition performance of locusts in an appetitive-conditioning paradigm[17] (**Supplementary Fig. 7a**). In this assay, we trained each locust to associate a conditioned stimulus (CST; hex or iaa or cit) with a grass reward (unconditioned stimulus) that followed the CST presentation (Online Methods). After six training trials, we evaluated the behavioral response of each trained locust in an unrewarded test phase. We used selective opening of the maxillary palps (sensory appendages close to the mouth area) to CST presentations during test trials as an indicator of acquired memory.

We found that the performance of trained locusts in unrewarded test trials remained consistent even when assessed using multiple test trials (**Supplementary Fig. 7b**). Taking advantage of this result, we tested each trained locust by presenting the following set of stimuli in a random order: (i) the conditioned odor (hex or iaa or cit), (ii) an untrained odor (2oct or bzald or ger) and (iii) the conditioned stimulus presented atop a background odor in each of the three dynamic states (**Fig. 1b**).

Among the three CSTs employed in our behavioral experiments, only hex and iaa resulted in effective associative learning (**Fig. 7** and **Supplementary Fig. 7c**). For these odors, nearly 70% of the locusts responded to the CST by opening their maxillary palps in anticipation of the reward. The palp-opening response (POR) to the CST presentations was significantly greater than the POR to an untrained odor ($P = 0.0052$ for hex-2oct and $P = 8.64 \times 10^{-7}$ for iaa-bzald, McNemar's exact tests Bonferroni corrected for multiple comparisons). We found that locusts responded rapidly to the conditioned odor with a median response latency of 0.58 s (i.e., the onset of a visually detectable movement of palps). More locusts responded to an untrained odor (2oct) that belonged to the same functional group as the CST (hex).

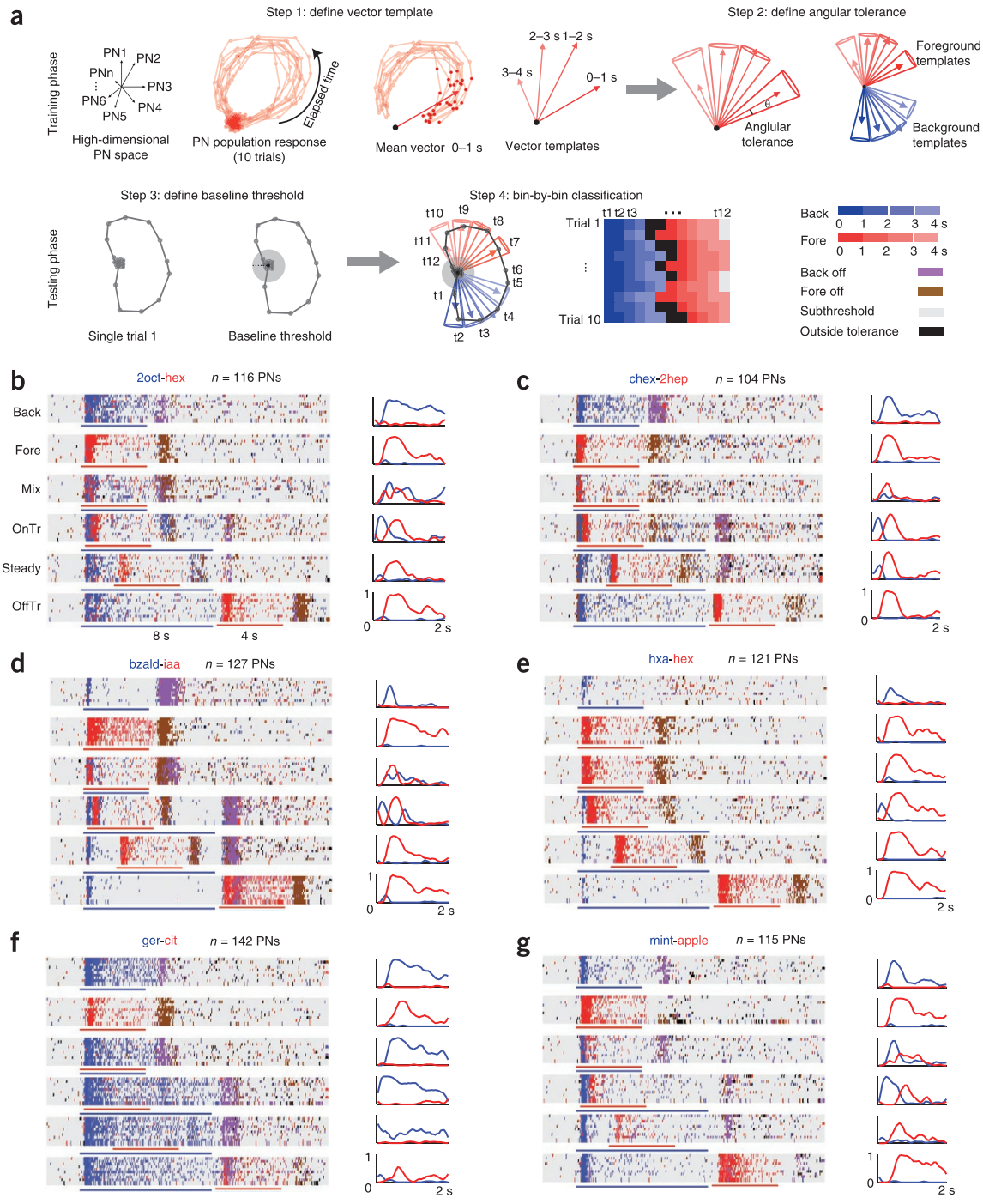

Figure 5 Projection neuron population response classification in a piecewise manner can allow background-independent recognition of odors. (**a**) Classification analysis, in which high-dimensional projection neuron activity patterns were first obtained during pure odor presentations and used to construct reference template vectors for each background and foreground odor. Five trial-averaged reference templates were constructed for each odor that represent the mean activity during the following time bins: 0–1 s, 1–2 s, 2–3 s and 3–4 s after odor onset and a 2-s window after stimulus termination. The classification analysis was restricted to quantify meaningful pattern matches using two parameters: angular tolerance and a detection threshold (Online Methods). Any trial not used to create the reference templates was regarded as a test trial. The odor-evoked activity patterns were categorized in the same odor class as their nearest reference template. Blue pixels indicate the proximity to the background odor templates, and red pixels indicate similarity with foreground odor responses. Subthreshold activities are indicated with gray pixels, and any projection neuron activity patterns outside an angular distance tolerance limit are indicated by black pixels. This analysis was repeated for all time bins in a test trial. (**b**–**g**) Classification results for all background-foreground odor pairs. Each panel shows six classification blocks corresponding to the stimulation conditions shown in **Figure 1b**. The odor identities (blue, background; red, foreground), number of projection neurons (which are the same as in **Fig. 4**) and presentation durations are shown. A leave-one-trial-out scheme was followed for the classification of pure foreground and background odor trials. The graphs on the right show the classification probabilities for each time bin (i.e., the percentage of blue or red pixels for a given time bin) during the first 2 s after foreground odor onsets (and after background odor onset when presented alone; first block).

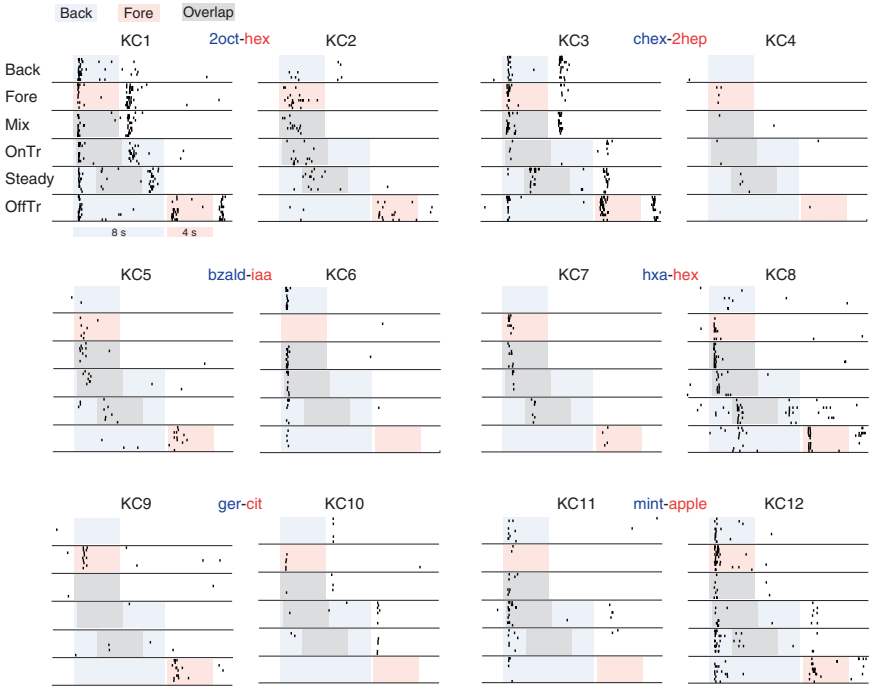

Figure 6 Kenyon cells are sensitive to partial pattern matches in antennal lobe activity. Shown are raster plots of the responses of 12 different Kenyon cells (KC1–KC12) to each background-foreground odor combination. Each Kenyon cell raster plot is arranged according to the scheme described in **Figure 1b**.

How well do trained locusts recognize CST introductions that followed the untrained odor with varying latencies? Two orthogonal predictions can be made from our physiology data. If any pattern match in the spatiotemporal responses was sufficient for recognition, then we would expect both hex and iaa to be recognized correctly even when coming after another stimulus. However, if a precise match between odor-evoked activities was required, then none of those introductions should elicit a behavioral response. We found that trained locusts were able to show PORs to conditioned odors irrespective of how they were introduced (**Fig. 7a**,**b** and **Supplementary Fig. 7d**,**e**).

Next we examined whether pattern matches in ensemble projection neuron responses predict locust PORs in the behavioral assay. To this end, for both conditioned odors (hex and iaa), we plotted the classification probability for each stimulus used during the testing phase against their POR probability (**Fig. 7c**). For this analysis, we computed projection neuron firing pattern similarities only with respect to the foreground odor response templates (Online Methods). We observed a significant correlation between our classification results and the behavioral data (regression analysis, $R^2 = 0.6982$, $P = 0.0026$; $n = 10$ data points). Hence, this result reveals a direct relationship between dynamic processing of odor signals in the antennal lobe and recognition performance of locusts in a behavioral task.

We found that although citral was not suitable as a conditioned odor in the appetitive-conditioning assay, this odor repelled locusts in a T-maze assay (**Fig. 8a**, **Supplementary Fig. 7f** and Online Methods). Fortuitously, the corresponding background odor used in our physiology experiments (geraniol) elicited an exact opposite innate response and functioned as an attractant in the T-maze assay. Both our dimensionality reduction analysis and classification results revealed that the geraniol responses masked any subsequent citral introductions when these two odors were presented in an overlapping fashion. This result suggests that a mixture of these two odors should attract locusts in the T-maze assay (**Fig. 8b**). We tested this prediction by presenting citral 2 s after geraniol introduction and found that locusts were indeed attracted toward the T-maze arm that delivered this stimulus (**Fig. 8a**; $P < 0.05$, exact binomial test with Bonferroni correction for multiple comparisons; $n = 20$ locusts for each test stimulus).

Hence, integrating our physiology results with behavioral data, we conclude that ensemble projection neuron firing patterns underlie both acquired as well as innate preferences in this olfactory system.

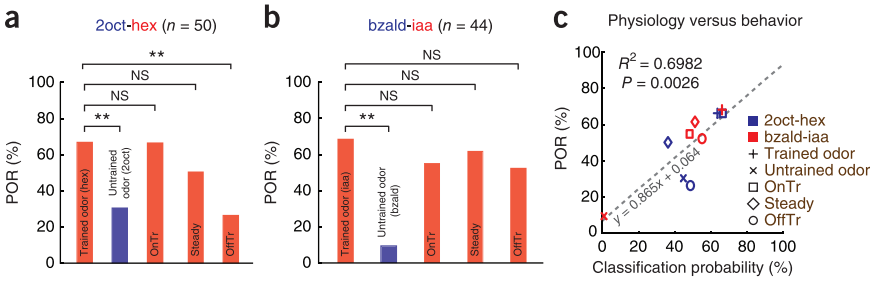

Figure 7 Behavioral ability of locusts to recognize odorants independently of background correlates with the classification analysis results. (**a**) Bar graph summarizing the PORs of $n = 50$ locusts during the testing phase. Each locust used in the assay was tested with the following set of stimuli presented in a random order: the trained odor (hex; CST), an untrained odor (2oct) and introductions of CST when the background odor (2oct) response was in its on-transient, steady-state or off-transient phase. Of note, the response to the CST was significantly higher than that observed during untrained odor exposures (**$P = 0.0052$, McNemar's exact test with Bonferroni-corrected P values for multiple comparisons). A substantial percentage of locusts responded to the CST regardless of when it was presented (NS, not significant, $P > 0.1$, McNemar's exact test with Bonferroni-corrected P values). However, the PORs to CST during off-transient introductions were significantly lower than the responses observed for the same CST presented alone (**$P = 2.289 \times 10^{-5}$, McNemar's exact test with Bonferroni-corrected P values for multiple comparisons). (**b**) Similar plots showing PORs for the bzald-iaa odor combination ($n = 44$ locusts). Here iaa was used as the CST, and bzald was the untrained odor. The POR to the CST was significantly higher than that observed during untrained odor exposures (**$P = 8.64 \times 10^{-7}$, McNemar's exact test with Bonferroni correction). No difference in the POR to CST was observed between iaa presented alone and introductions that happened during different dynamic phases of bzald activity (NS, $P > 0.4$, McNemar's exact test with Bonferroni correction). (**c**) POR probabilities plotted against the classification probabilities obtained from our quantitative classification analysis of high-dimensional projection neuron response patterns. A regression analysis (dashed line) revealed that the correlation between our physiology results and behavioral data was significant ($R^2 = 0.6982$, $P = 0.0026$, d.f. = 8; $n = 10$ data points).

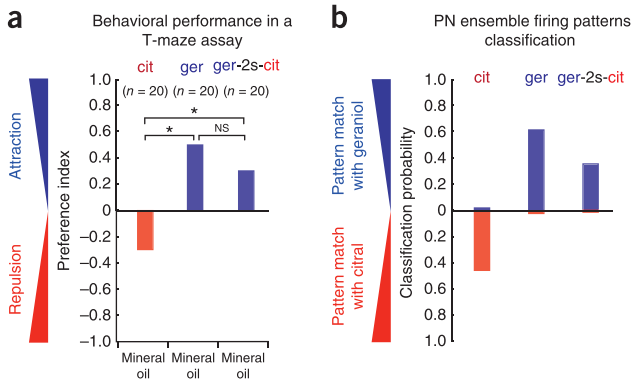

Figure 8 Behavioral results validate the predictions from our physiology data. (**a**) Results from a T-maze assay (Online Methods). Each locust was given 4 min to make a decision: select a T-maze arm and reach and touch the sidewall at the end of the selected arm with its leg or antenna. The bar plots show the preferences of the locusts to the three test stimuli delivered: citral alone, geraniol alone or geraniol, a 2-s lag and then citral. The preference index is defined as the percentage of locusts choosing the odor arm minus the percentage choosing the mineral oil arm. Overall, locusts were repelled by citral but attracted by geraniol and the geraniol-citral odor sequence. The responses to geraniol and the geraniol-citral sequence were both significantly different from the citral response (exact binomial test, $*P < 0.05$ with Bonferroni correction for multiple comparisons; NS, $P = 0.6427$; $n = 20$ locusts for each case). (**b**) Projection neuron classification probabilities for the same set of stimuli used in the T-maze experiments (the mean classification probability was computed from the curves shown on the right in **Fig. 5f**).

DISCUSSION

We examined how a spatiotemporal coding mechanism allows an olfactory system to detect and recognize olfactory cues in the presence of another competing stimulus. Our results revealed that the responses of ORNs to an odorant changed when the same stimulus was presented along with or after another stimulus. Subsequent processing of these inconsistent sensory inputs varied depending on the latency with which the fresher stimuli were introduced. However, we found that after most of the foreground odor introductions, the antennal lobe ensemble activity restructured to create neural activity that overlapped across different presentation conditions. Piecewise decoding of these responses by Kenyon cells allowed robust detection of any similarity in the antennal lobe ensemble activity.

Our study also examined when the olfactory system achieved the ability to process a newer stimulus independently of its recent stimulus history. This is important because in most natural settings, the latency with which a fresh odorant is received cannot be controlled. Therefore, we presented the newer stimulus during all possible dynamic states of neural activity elicited by a preceding odor. For cases when the onsets of the two odors happened within a few hundred milliseconds of each other, neither the sensory input from the ORNs[21,35,36] nor the behavioral response would have attained complete adaptation (although behavioral responses can change extremely rapidly[37,38]). Nevertheless, our results revealed that when encountered after another odorant, either all introductions of fresher stimuli were tracked independently of the latency with which they were introduced or none of them were tracked.

We found that rapid filtering of background odor signals began at the level of the ORNs. A lengthy odor pulse did not elicit a similarly lengthy response in all ORNs. A subset of ORNs showed a transient response that was substantially reduced within a second after odor onset, whereas another subset showed a response that persisted for the complete duration of the odor pulse (**Fig. 2a**). Because the same odor could elicit both transient and persistent responses in different subsets of ORNs, these temporal response properties cannot be explained by variations in stimulus dynamics alone[39]. These results suggest that rapid adaptation at the level of sensory neurons may contribute to filtering of background stimuli and facilitate the detection of new odor introductions.

We found that both individual ORN firing activity and bulk electroantennogram signals were insufficient to predict responses in downstream projection neurons. An odor that elicited a weak electroantennogram response sometimes generated a strong projection neuron population response (for example, 2oct; **Supplementary Figs. 1** and **2**). We observed the converse situation in some cases (for example, bzald). Furthermore, we found that even though spiking activity in individual ORNs was greater, when we presented overlapping pairs of stimuli, individual projection neuron responses to these blends were lower than the responses to the foreground stimulus presented alone (**Fig. 3b**). Surprisingly, during off-transient introductions of foreground odors, a relatively weaker ORN input was able to elicit a comparatively stronger projection neuron firing activity. Our behavior results also reveal that in some cases, the off-transient activity that is due to a background stimulus could interfere with subsequent odor recognition (**Fig. 7a**; hex-2oct; $P = 2.289 \times 10^{-5}$, McNemar's exact tests with Bonferroni correction for multiple comparisons; $n = 50$ locusts). These results suggest that sensory neuron activity alone is insufficient to completely understand the responses generated in the following circuits.

We found that the responses of a large subset of projection neurons to the foreground odor remained unaffected because of changes in stimulus history (~36% of responsive cells; data not shown). Such a projection neuron subset existed even for the ger-cit odor pair, for which none of the citral introductions were effectively tracked by the ensemble projection neuron activity. Hence, we conclude that the existence of this subset, though necessary, was insufficient by itself to ensure that the ensemble activity overlapped across conditions.

Most of our projection neuron analyses discussed here rely on pooling data across multiple locusts. Did this analysis approach affect our conclusions? Several lines of evidence point to the fact that pooling data would lead to more meaningful interpretation of the data set, as it does not suffer from subsampling effects. Empirically, in agreement with previous studies[22,24], we found that our classification results converged when using roughly 80 projection neurons (data not shown). Furthermore, Monte-Carlo simulations revealed that the probability of double counting a stereotypic projection neuron across locusts (if any existed) was extremely low. In addition, classification results when using only those projection neurons recorded from individual locusts (with both antennal lobes included) qualitatively matched our overall results (**Supplementary Fig. 8**). Therefore, we expect this pooling strategy to be well founded for the objectives of this study.

We found that for all odor pairs, a subset of Kenyon cells responded to any overlap observed in the antennal lobe ensemble activity. Even for those foreground odors where the overlap across conditions occurred in nonidentical response segments (for example, the 2oct-hex trajectories shown in **Fig. 4**), we found Kenyon cells that responded in an invariant manner (**Fig. 6**; KC1 and KC2). We also found a few Kenyon cells that responded to only a subset of overlapping conditions (**Fig. 6**; ger-cit). Such Kenyon cell responses were still consistent with the classification analysis results for that odor pair. Hence, our data support the existing interpretation of Kenyon cells as a piecewise decoder of ensemble projection neuron activity[24,29].

Our physiology results alone were not sufficient to identify the attributes of spatiotemporal ensemble activity that allow for background-independent recognition of odors. Given these results, several possible behavioral outcomes can be anticipated. For example, because an exact match between

the entire set of spatiotemporal responses was not achieved in any of the CST presentation conditions, one possible outcome is that locusts will not recognize subsequent introductions of a trained odor after a distractant. Alternately, whether or not neural activity returned to baseline levels before the onset of a fresher stimulus (i.e., temporal decoupling) may be important for robust recognition. If the latter case is indeed true, then we would expect a difference in recognition performance between on-transient and steady-state introductions of the same CST. Notably, our behavior results appear to indicate a rather simple approach. Any partial pattern match with or without a reset in neural activity was sufficient for recognition of CST by trained locusts (**Fig. 7**).

In conclusion, our results reveal that an odorant evokes only certain combinations of ensemble neural activity in the antennal lobe that encodes for its identity (a subspace or an attractor; **Supplementary Fig. 9a**). The neural response dynamics during on-transient and steady-state periods were both contained within this subspace for a given pure odor stimulation. When presented atop an ongoing background odor, a strong excitatory input appeared to be necessary to overcome the resistance offered by the ongoing neural activity and switch the population response from the background attractor to a different subspace that represented the foreground odor. This interpretation is supported by our projection neuron analysis (**Supplementary Fig. 9b**), which indicated that among all the foreground odors tested, citral evoked less excitatory and more inhibitory responses in most projection neurons. Furthermore, citral also elicited weaker projection neuron ensemble activity compared to geraniol (**Supplementary Fig. 1**). Hence, none of the citral introductions was properly tracked. Notably, we found that reaching any segment of the attractor was sufficient for robust recognition. Our Kenyon cell recordings indicate that such an encoding approach is ideally suited for a decoder that employs coincidence-detection mechanisms. Hence, our results provide a fundamental insight into a behaviorally important olfactory computation.

METHODS

Methods and any associated references are available in the online version of the paper.

Note: Any Supplementary Information and Source Data files are available in the online version of the paper.

ACKNOWLEDGMENTS

We thank N. Katta for performing double-blind behavior evaluation studies and D. Yang for help with behavioral experiments. We thank F. Gabbiani (Baylor College of Medicine), M. Stopfer and S. Reiter (Eunice Kennedy Shriver National Institute of Child Health and Human Development, US National Institutes of Health), D. Barbour, R. Wessel and members of Raman Lab (Washington University, St. Louis) for comments on previous versions of the manuscript. This research was supported by a McDonnell Center for Systems Neuroscience grant, an Office of Naval Research grant (N00014-12-1-0089) and startup funds from the Department of Biomedical Engineering at Washington University, St. Louis to B.R.

AUTHOR CONTRIBUTIONS

B.R. conceived the study and designed the experiments. D.S., K.L. and G.S. performed the electrophysiological recordings. C.L. and S.P. did the behavioral experiments. C.L., K.L. and D.S. analyzed the data. B.R. wrote the paper, and D.S., C.L. and K.L. provided feedback on the manuscript.

COMPETING FINANCIAL INTERESTS

The authors declare no competing financial interests.

1. Laurent, G., Wehr, M. & Davidowitz, H. Temporal representations of odors in an olfactory network. *J. Neurosci.* **16**, 3837–3847 (1996).
2. Meredith, M. & Moulton, D.G. Patterned response to odor in single neurons of goldfish olfactory bulb: influence of odor quality and other stimulus parameters. *J. Gen. Physiol.* **71**, 615–643 (1978).
3. Di Lorenzo, P.M., Chen, J.Y. & Victor, J.D. Quality time: representation of a multidimensional sensory domain through temporal coding. *J. Neurosci.* **29**, 9227–9238 (2009).
4. Jones, L.M., Fontanini, A., Sadacca, B.F., Miller, P. & Katz, D.B. Natural stimuli evoke dynamic sequence of states in sensory cortical ensembles. *Proc. Natl. Acad. Sci. USA* **104**, 18772–18777 (2007).
5. Seifritz, E. *et al.* Spatiotemporal pattern of neural processing in the human auditory cortex. *Science* **297**, 1706–1708 (2002).
6. Smear, M., Shusterman, R., O'Conor, R., Bozza, T. & Rinberg, D. Perception of sniff phase in mouse olfaction. *Nature* **479**, 397–400 (2011).
7. Griffiths, T.D., Uppenkamp, S., Johnsrude, I., Josephs, O. & Patterson, R.D. Encoding of the temporal regularity of sound in the human brainstem. *Nat. Neurosci.* **4**, 633–637 (2001).
8. Ahissar, E., Haidarliu, S. & Zacksenhouse, M. Decoding temporally encoded sensory input by cortical oscillations and thalamic phase comparators. *Proc. Natl. Acad. Sci. USA* **94**, 11633–11638 (1997).
9. Carlson, B.A. Temporal-pattern recognition by single neurons in a sensory pathway devoted to social communication behavior. *J. Neurosci.* **29**, 9417–9428 (2009).
10. Machens, C.K. *et al.* Representation of acoustic communication signals by insect auditory receptor neurons. *J. Neurosci.* **21**, 3215–3227 (2001).
11. Schnitzer, M.J. & Meister, M. Multineuronal firing patterns in the signal from eye to brain. *Neuron* **37**, 499–511 (2003).
12. Friedrich, R.W. & Laurent, G. Dynamic optimization of odor representations by slow temporal patterning of mitral cell activity. *Science* **291**, 889–894 (2001).
13. Dayan, P. & Abbott, L.F. *Theoretical Neuroscience: Computational and Mathematical Modeling of Neural Systems* (The MIT Press, 2001).
14. Stopfer, M., Bhagavan, S., Smith, B.H. & Laurent, G. Impaired odour discrimination on desynchronization of odour-encoding neural assemblies. *Nature* **390**, 70–74 (1997).
15. Vickers, N.J., Christensen, T.A., Baker, T.C. & Hildebrand, J.G. Odour-plume dynamics influence the brain's olfactory code. *Nature* **410**, 466–470 (2001).
16. Ito, I., Ong, R.C., Raman, B. & Stopfer, M. Sparse odor representation and olfactory learning. *Nat. Neurosci.* **11**, 1177–1184 (2008).
17. Simões, P., Ott, S.R. & Niven, J.E. Associative olfactory learning in the desert locust, *Schistocerca gregaria*. *J. Exp. Biol.* **214**, 2495–2503 (2011).
18. Kreher, S.A., Matthew, D., Kim, J. & Carlson, J.R. Translation of sensory input into behavioral output via an olfactory system. *Neuron* **59**, 110–124 (2008).
19. Galán, R.F., Sachse, S., Galizia, C.G. & Herz, A.V.M. Odor-driven attractor dynamics in the antennal lobe allow for simple and rapid olfactory pattern classification. *Neural Comput.* **16**, 999–1012 (2004).
20. Mazor, O. & Laurent, G. Transient dynamics versus fixed points in odor representations by locust antennal lobe projection neurons. *Neuron* **48**, 661–673 (2005).
21. Raman, B., Joseph, J., Tang, J. & Stopfer, M. Temporally diverse firing patterns in olfactory receptor neurons underlie spatiotemporal neural codes for odors. *J. Neurosci.* **30**, 1994–2006 (2010).
22. Stopfer, M., Jayaraman, V. & Laurent, G. Odor identity vs. intensity coding in an olfactory system. *Neuron* **39**, 991–1004 (2003).
23. Bathellier, B., Buhl, D.L., Accolla, R. & Carleton, A. Dynamic ensemble coding in the mamallian olfactory bulb: sensory information at different timesales. *Neuron* **57**, 586–598 (2008).
24. Brown, S.L., Joseph, J. & Stopfer, M. Encoding a temporally structured stimulus with a temporally structured neural representation. *Nat. Neurosci.* **8**, 1568–1576 (2005).
25. Rinberg, D., Koulakov, A. & Gelperin, A. Speed-accuracy tradeoff in olfaction. *Neuron* **51**, 351–358 (2006).
26. Uchida, N. & Mainen, Z. Speed and accuracy of olfactory discrimination in the rat. *Nat. Neurosci.* **6**, 1224–1229 (2003).
27. Abraham, N.M. *et al.* Maintaining accuracy at the expense of speed: stimulus similarity defines odor discrimination time in mice. *Neuron* **44**, 865–876 (2004).
28. Ditzen, M., Evers, J. & Galizia, C.G. Odor similarity does not influence the time needed for odor processing. *Chem. Senses* **28**, 781–789 (2003).
29. Broome, B.M., Jayaraman, V. & Laurent, G. Encoding and decoding of overlapping odor sequences. *Neuron* **51**, 467–482 (2006).
30. Spors, H., Wachowiak, M., Cohen, L.B. & Friedrich, R.W. Temporal dynamics and latency patterns of receptor neuron input to the olfactory bulb. *J. Neurosci.* **26**, 1247–1259 (2006).
31. Spors, H. & Grisvald, A. Spatio-temporal dynamics of odor representations in the mammalian olfactory bulb. *Neuron* **34**, 301–315 (2002).
32. Ito, I., Bazhenov, M., Ong, R.C., Raman, B. & Stopfer, M. Frequency transitions in odor-evoked neural oscillations. *Neuron* **64**, 692–706 (2009).
33. Roweis, S.T. & Saul, L.K. Nonlinear dimensionality reduction by locally linear embedding. *Science* **290**, 2323–2326 (2000).
34. Perez-Orive, J. *et al.* Oscillations and sparsening of odor representations in the mushroom body. *Science* **297**, 359–365 (2002).
35. De Palo, G. *et al.* Common dynamical features of sensory adaptation in photoreceptors and olfactory sensory neurons. *Sci. Rep.* **3**, 1251 (2013).
36. Nagel, K.I. & Wilson, R.I. Biophysical mechanisms underlying olfactory receptor neuron dynamics. *Nat. Neurosci.* **14**, 208–216 (2011).
37. Baker, T.C. & Haynes, K.F. Field and laboratory electroantennographic measurements of pheromone plume structure correlated with oriental fruit moth behaviour. *Physiol. Entomol.* **14**, 1–12 (1989).
38. Laing, D.G., Eddy, A., Francis, G.W. & Stephens, L. Evidence for the temporal processing of odor mixtures in humans. *Brain Res.* **651**, 317–324 (1994).
39. Martelli, C., Carlson, J.R. & Emonet, T. Intensity invariant dynamics and odor-specific latencies in olfactory receptor neuron response. *J. Neurosci.* **33**, 6285–6297 (2013).

ONLINE METHODS

Odor stimulation. Odorants were delivered using a standard protocol described in an earlier work[24]. Briefly, odor solutions were diluted in mineral oil to 1% concentration (vol/vol) and placed in 60-ml glass bottles. Odor pulses were delivered by injecting a constant volume (0.1 l per min) of the static headspace above the odorants into a desiccated air stream (0.75 l per min) flowing continuously across the antenna. A large vacuum funnel was placed behind the locust preparation to continuously remove the delivered odorants. The following odorants were used in this study: 2-octanol, hexanol, cyclohexanone, 2-heptanone, benzaldehyde, isoamyl acetate, hexanal, geraniol, citral, peppermint and apple. Each stimulus was presented multiple times in one or two pseudorandomized blocks of five or ten trials each (five trials for ORN recordings and ten trials for projection neuron and Kenyon cell recordings). The interstimulus interval was at least 60 s for all recordings.

Electrophysiology. Electrophysiological experiments were conducted using locusts (*Schistocerca americana*) raised in a crowded colony. Young adults (after the fifth instar) of either sex were used. ORN recordings were made from different sensilla types in intact but immobilized locust antennae as described previously[21]. The antenna was stabilized using wax, and a reference electrode (Ag/AgCl wire) was inserted into the locust gut. Single sensillum recordings were made using saline-filled glass micropipettes (~10-µm diameter, 5–10 MΩ) that were inserted into the base of the sensillum. Acquired signals were amplified using a differential amplifier (Grass P55), filtered between 0.3 and 10.0 kHz and acquired at a 15-kHz sampling rate (PCI-MIO-16E-4 DAQ cards, National Instruments). Multiunit single sensillum recordings were spike sorted offline using Spike-o-Matic software[40] implemented in IGOR Pro (Wavemetrics).

To monitor activity in the antennal lobe and mushroom body, locusts were immobilized with both antennae intact, and the brain was exposed, desheathed and superfused with locust saline at room temperature[1]. In the antennal lobe, multiunit tetrode recordings were made using 16-channel, 4 × 4 silicon probes (NeuroNexus). Similar recordings were made in the mushroom body by inserting custom-made twisted wire tetrodes (nickel chromium wire, RO-800, Kanthal Precision Technology). Kenyon cell recordings were made from the superficial layers of the mushroom body that only contains Kenyon cell somata[34]. Mushroom body recording sites were selected by determining whether a particular location yielded any Kenyon cells that responded to at least one of the odors tested (background or foreground). All multiunit electrodes were electroplated with gold to obtain impedances in the 200–300 kΩ range. A custom-made 16-channel amplifier (Biology Electronics Shop, Caltech, Pasadena, CA) was used to collect both projection neuron and Kenyon cell data at 15 kHz. The data were amplified at a 10,000 gain, filtered between 0.3 and 6 kHz ranges and saved using a LabView data acquisition system. To allow the assignment of recorded spikes to unique cell sources, spike sorting was done offline using the best three or four channels recorded and conservative statistical principles. Examples of ORN, projection neuron and Kenyon cell spike sorting are shown in **Supplementary Figure 10**.

A visual demonstration of these multiunit extracellular recording techniques is available online[41].

Electroantennogram recordings were made using intact locust antenna. 3–4 distal antennal segments were cut in order to insert an Ag/AgCl wire. A ground electrode was inserted into the contralateral eye. The signals were acquired using a direct-coupled amplifier (Brownlee Precision).

ORN, projection neuron, Kenyon cell spike sorting. In our single sensillum recordings, spiking events were identified as voltage peaks above a preset threshold (usually 2–5 times the noise s.d.). We noticed that the ORN spike amplitude could change somewhat as the ORNs adapted to odors. To deal with this issue, while sorting these ORN spikes, we allowed each cell cluster to include events of variable amplitude as long as different sorted units remained well separated (by at least five times the noise s.d.). Additionally, to be considered single units, less than 20% of spikes associated with the identified unit were allowed to have an interspike interval of less than 20 ms. A similar procedure was followed for projection neuron and Kenyon cell spike sorting. Here, the best four channels were chosen from the multielectrode array for spike-sorting purposes. To identify single units, the following criteria were used: cluster separation >5 noise s.d., number of spikes within 20 ms <6.5% and spike waveform variance <6.5 noise s.d. A total of 119 ORNs (recorded from 27 locusts), 725 projection neurons (recorded from 70 locusts) and 99 Kenyon cells (recorded from 39 locusts) were identified using this approach.

PSTHs. Spike trains of each ORN, projection neuron and Kenyon cell were segmented into 100-ms nonoverlapping time bins, summed and smoothed by a three- or five-point average zero-phase digital filter. Averages across trials and cells were computed to obtain the population-level PSTHs shown in **Figure 1a** and **Supplementary Figures 1** and **6**.

Spike count comparison of individual ORNs and projection neurons. All analyses involving spike counts were done using cells with an excitatory response. The following two independent criteria[34] had to be satisfied for a neuron's response to be considered excitatory: (i) amplitude criterion: the odor-evoked neural firing activity (averaged over trials) in at least one of the time bins during odor presentation must have exceeded 6.5 s.d. of baseline activity (average activity during a 2-s prestimulus window); and (ii) reliability criterion: the amplitude criterion must have been met in 50% of trials. The amplitude and reliability criteria had to be met in at least one of the six stimulus presentation conditions shown in **Figure 1b** for the cell to be included in this analysis.

Spike counts for cells satisfying both the amplitude and reliability criteria were computed in a 2-s window after the foreground odor was presented either alone or after a background odor. Comparisons were made between spike counts across conditions (no background as compared to background) for each ORN and projection neuron using one-way ANOVA at $P < 0.05$. Bonferroni correction was applied to account for multiple comparisons.

Trajectory analysis. For this analysis, we first arranged the ensemble projection neuron responses as time series data of n dimensions (where n is number of neurons recorded) and m steps (the number of 50-ms time bins, where $m = 80$). Only the 4 s of projection neuron activity during the presentation of a single odor or foreground stimulus were used for this analysis. Dimensionality reduction was performed using the LLE technique[33] (Matlab code obtained from http://www.cs.toronto.edu/~roweis/lle was used). The low-dimensional points were connected in a temporal order to visualize neural response trajectories to different stimuli. Qualitatively similar trajectories were generated for a wide range of neighborhood values (k = 10–35; data not shown). The plots shown in **Figure 4a–f** were generated with k = 15, 13, 16, 15, 33 and 11, respectively. Of note, the LLE analysis results were similar to those obtained using a linear principal components analysis (**Supplementary Fig. 3**).

Classification analysis of projection neuron ensemble responses. We considered ensemble projection neuron spike counts in a 50-ms nonoverlapping time bin as a high-dimensional response vector. Response vectors obtained during solitary foreground and background odor exposures were regarded as the desired reference templates to be pattern matched. Five trial-averaged reference templates were generated for each odor (4-s pulse duration). These reference templates represented the mean ensemble projection neuron activity during the following temporal response segments: four 1-s windows after odor onset (0–1 s, 1–2 s, 2–3 s and 3–4 s) and a 2-s window after odor offset.

Ensemble projection neuron spike counts in trials that were not used to create reference templates were regarded as test response patterns to be categorized. To identify meaningful response patterns, we defined two criteria. First, we defined a threshold length that must be exceeded by a vector to be considered an odor-evoked response. The threshold was set as the mean length of the prestimulus activity vectors +2 s.d. Second, we defined a tolerance threshold that would restrict the classification analysis to include only those vectors that are within a certain angular distance (an 85° angular distance threshold was used for all classification analyses) to any one of the desired response templates. Angular distances between a given test vector ($\mathbf{V_t}$) and each reference vector ($\mathbf{V_r}$) was computed as follows:

$$\text{angular distance} = \cos^{-1}\left(\frac{\mathbf{V_t}\cdot\mathbf{V_r}}{|\mathbf{V_t}||\mathbf{V_r}|}\right)$$

Only those test vectors that exceeded the detection threshold but were within the defined tolerance threshold were classified. Each test vector was assigned to

doi:10.1038/nn.3570

the same odor category as its best matching reference template, background or foreground (color coded as blue or red pixels).

For classifying trials that involved pure background or foreground odor presentations, we followed the leave-one-trial-out validation approach. In other words, nine trials were used as training trials for constructing the reference templates, and the excluded trial became the test trial. This was repeated ten times such that each of the ten trials was made a test trial once.

For the linear regression analysis shown in **Figure 7c**, pattern matches with only the foreground odor reference templates were determined and plotted. We found that the result was robust ($R^2 > 0.46$, $P < 0.05$) for a wide range of angular tolerance threshold values ($65° \leq \theta \leq 85°$). The correlation results shown in **Figure 7c** were determined with $\theta = 75°$.

Significance analyses. Two metrics were defined to assess the significance of obtained classification results. First, baseline misclassification rates were determined as the percentage of time bins (averaged across trials) during the 2-s prestimulus baseline period that were classified (**Supplementary Fig. 5a**). The probability of classification during prestimulus periods was less than 5%. Second, vector templates experimentally obtained for all six odor pairs were used to ascertain classification rates when a large number of randomly generated unit vectors (100,000 vectors) were made as the test set. These 100,000 vectors were distributed such that their mean was chosen to be at 90° from the mean reference vectors (during odor presentations). Individual random vectors were obtained by adding a unit s.d. noise to the mean vector. Only ~5% of the generated random vectors were within the tolerance limit by chance. All other vectors exceeded the tolerance threshold and were not classified into any odor category (**Supplementary Fig. 5c**).

Inhibitory projection neuron response categorization. The same criteria used to determine an excitatory projection neuron response for the spike count comparisons were followed here (**Supplementary Fig. 9b**). We detected an inhibitory projection neuron response using the following two conditions: (i) amplitude criterion: odor-evoked neural firing rates (averaged over trials) do not exceed 2 s.d. of baseline activity (2-s prestimulus activity averaged over trials) in any time bin during odor presentation, and further, the mean firing rate during the entire stimulus duration must be lower than the mean baseline activity; and (ii) reliability criterion: the amplitude criterion must be met in 50% of trials.

Responsive Kenyon cell categorization. A Kenyon cell was considered to be responsive to an odor stimulus if it responded with at least one spike during the odor presentation period in four or more trials (out of the total ten trials).

Behavior experiments. Behavioral experiments were carried out by adapting a protocol described in an earlier work[17]. Adult locusts of either sex were starved for 24 h before the experiments. Locusts were immobilized within a plastic tube such that only the antenna and mouthparts were freely movable. Both compound eyes were closed using black electrical tape to reduce the influence of visual cues on behavior and reduce spontaneous activity. For all experiments, we used the following odorants as the CST: hexanol, isoamyl acetate and citral. Wheat grass was used as the unconditioned stimulus. The odor delivery setup was identical to that in our electrophysiology experiments. A video camera (Microsoft webcam) was used to capture the behavioral responses of locusts during the training and test trials, and these responses were analyzed in a double-blind manner. A light-emitting diode was used to signal the onset of odor and the duration of odor delivery in the video clip.

Six trials were used to train each locust to associate the conditioning stimulus with the food reward. During each training trial, a 10-s CST was presented first, which was followed by a grass reward (unconditioned stimulus) that was offered 4 s after CST onset. The intertrial interval was set to 10 min. To exclude any preconditioning to the CST, locusts that responded to the CST in the first training trial were eliminated from further experiments (<15%). Only those locusts that accepted the reward in at least four out of six training trials were used for testing (>80%).

Selective opening of maxillary palps to the CST presentation was used as an indicator of the acquired memory. The POR was considered positive if the locusts opened one or both of their maxillary palps, crossing an imaginary response threshold (red dashed line in **Supplementary Fig. 7a**) formed by the lateral groove of the labrum at least once during odor (4 s) presentation.

We first assessed whether the associative learning of a CST established during training was retained afterwards. We performed four successive retention tests at 10 min, 40 min, 70 min and 100 min after the last training trial. In each block of these retention tests, both trained (iaa) and untrained (bzald) odors were presented with a 10 min interval without any reward. **Supplementary Figure 7b** shows that the conditioned locusts had a significantly higher POR to the trained odor than the untrained odor (**$P = 1.22 \times 10^{-4}$ (retention test 1), 6.10×10^{-5} (retention test 2), 7.63×10^{-5} (retention test 3) and 3.05×10^{-5} (retention test 4); McNemar's exact test, $n = 28$ locusts). The relative percentages of locusts that showed a POR to the trained and untrained odor across multiple tests remained consistent (Cochran's Q test; CST, $Q = 0.67$, d.f. = 3, $P = 0.87$; untrained odor, $Q = 2.2$, d.f. = 3, $P = 0.53$).

We then assessed whether locusts that exhibited a selective POR to the CST were able to recognize the trained odor when it was presented during different dynamic states of a background odor. The stimulation protocol and odor pairs used were identical to those used in our electrophysiology experiments. A total of four consecutive retention tests were performed at 10 min, 40 min, 70 min and 100 min after the last training trial. These test trials comprised the following set of stimuli presented in a random order: (i) the conditioned odor, (ii) an untrained odor and (iii) the conditioned stimulus introduced during on transients, steady states and off transients of the background odor activity (**Fig. 1b**).

T-maze assay. A T-maze arena was designed with the following dimensions: 20 cm wide, 48 cm long and 22 cm high (a design adapted from an earlier work[17]). An elevated T bar (11 cm off the ground) was positioned centrally in this arena. The T bar was composed of two wooden rods measuring 44 cm and 7 cm in length. The shorter side arm split the longer rod into two arms of equal length. Locusts were kept restrained in a custom-designed holder that was located in the shorter side arm of the T bar. Two odor delivery ports (each 0.5 cm in diameter) were located on the sidewalls in line with the two arms of the T bar. An 8 cm × 8 cm square vent right behind the locust holder housed a 5V exhaust fan. The exhaust fan ensured that there was a stable air flow inside the maze. The flow patterns were visually confirmed with titanium tetrachloride fumes. A transparent plexiglass lid was used to prevent locusts from escaping from the arena. A camera was used to record the movements of the locusts within the T maze.

Locusts were selected using procedures similar to those used in our electrophysiology experiments. Locusts were starved for 24 h before the experiments. Locusts were initially kept restrained in a custom-designed locust holder and released just before odor delivery. A test odor (1% concentration (vol/vol)) and the control odor (mineral oil) were simultaneously presented at the two odor delivery ports. A 4-min odor pulse was delivered by injecting a constant volume (0.1 l per min) of the static headspace above the odorants and mineral oil into a desiccated air stream (0.2 l per min). To prevent depletion of headspace in the odor bottles, stimulus delivery was programmed to seamlessly switch between two equivalent odor bottles every 12 s.

Locusts were given 4 min to make a decision: select a T-maze arm and then reach and touch the sidewall at the end of the selected arm with its leg or antenna. The overall locust preference in the T maze was quantified as follows:

$$\text{Preference index} = \frac{\text{Number of locusts moving towards the odor} - \text{number of locusts moving away from the odor}}{\text{Total number of locusts (towards + away)}}$$

Locusts that did not choose a T-maze arm or went off of them were discarded from the final analysis (<20% of the total locusts). Statistical comparisons were performed using an exact binomial test with Bonferroni correction for multiple comparisons at a 0.05 confidence level.

Each locust used in our T-maze experiments was used only for one trial. The entire T maze was cleaned with ethyl alcohol between trials to prevent any conspecific cues from the previous trial from influencing the overall results. Further, the test odor and control odor ports were chosen randomly for each trial to prevent any directional bias from influencing our results.

Locusts were kept on a 12-h day, 12-h night cycle (where 7 a.m. to 7 p.m. was day). All behavioral experiments were performed between 9 a.m. and 3 p.m.

Justifications for sample size and statistical tests used. All statistical significance tests done in the manuscript were two sided. Bonferroni-corrected *P* values were used for all multiple comparisons.

No statistical methods were used to predetermine sample sizes, but our sample sizes are similar to those reported in previous publications in the field[22–24,29]. For behavioral experiments, we used a sample size that was large enough to demonstrate statistical significance. Even in cases where statistical significance was achieved with a smaller sample size, we used $n = 20$ locusts.

For the one-way ANOVA analysis and paired *t* tests, the normality of the data set was confirmed using the Jarque-Bera test. We also examined the equal variance assumption using Bartlett's test. The equal variance assumption was met in ~80% of ORNs and ~70% of projection neurons studied (at a $P = 0.01$ significance level).

Linear regression analysis assumes that data can be fit using a straight line and sample points are independent of each other, both of which were satisfied in our case.

McNemar's exact test was used for statistical comparison of PORs of the same locust under different conditions (nominal data with matched pairs of subjects). Cochran's *Q* test was used to compare the performance of locusts in four back-to-back retention tests (**Supplementary Fig. 7b**). This is an extension of McNemar's exact test for $k > 2$ experiments.

An exact binomial test was used to statistically compare the distribution of locusts that went toward or away from the odorant delivered. For these tests, the sample sizes were small ($n = 20$), the trials were independent (different locusts were used for each trial) and the probability of success was constant.

40. Pouzat, C., Mazor, O. & Laurent, G. Using noise signature to optimize spike-sorting and to assess neuronal classification quality. *J. Neurosci. Methods* **122**, 43–57 (2002).
41. Saha, D., Leong, K., Katta, N. & Raman, B. Multi-unit recording methods to characterize neural activity in the locust (*Schistocerca americana*) olfactory circuits. *J. Vis. Exp.* **71**, pii: e50139 (2013).

doi:10.1038/nn.3570